Phenomenology of nonuniversal gaugino masses in supersymmetric grand unified theories

Katri Huitu,[1,2,*] Jari Laamanen,[1,2,†] Pran N. Pandita,[3,‡] and Sourov Roy[2,§]

[1]*High Energy Physics Division, Department of Physical Sciences, P.O. Box 64, FIN-00014 University of Helsinki, Finland*
[2]*Helsinki Institute of Physics, P.O. Box 64, FIN-00014 University of Helsinki, Finland*
[3]*Department of Physics, North-Eastern Hill University, Shillong 793 022, India*

(Received 11 February 2005; published 16 September 2005)

Grand unified theories can lead to nonuniversal boundary conditions for the gaugino masses at the unification scale. We consider the implications of such nonuniversal boundary conditions for the composition of the lightest neutralino as well as for the upper bound on its mass in the simplest supersymmetric grand unified theory based on the $SU(5)$ gauge group. We derive sum rules for neutralino and chargino masses in different representations of $SU(5)$ which lead to different nonuniversal boundary conditions for the gaugino masses at the unification scale. We also consider the phenomenological implications of the nonuniversal gaugino masses arising from a grand unified theory in the context of large hadron collider. In particular we investigate the detection of heavy neutral Higgs bosons H^0, $A^0$from H^0, $A^0 \to \tilde{\chi}_2^0 \tilde{\chi}_2^0 \to 4l$ and study the possibilities of detecting the neutral Higgs bosons in cascade decays, including the decays $\tilde{\chi}_2^0 \to h^0(H^0, A^0)\tilde{\chi}_1^0 \to b\bar{b}\tilde{\chi}_1^0$.

DOI: 10.1103/PhysRevD.72.055013 PACS numbers: 12.60.Jv, 11.30.Er, 14.80.Ly

I. INTRODUCTION

Supersymmetry is at present an attractive framework in which the Higgs sector of the standard model (SM), so crucial for its consistency, is technically natural. It is widely expected that some of the supersymmetric partners of the SM particles will be produced at the CERN large hadron collider (LHC) which is going to start operation in a few years. In the experimental search for supersymmetry (SUSY) the lightest supersymmetric particle will play a crucial role since the heavier supersymmetric particles will decay into it. In SUSY models with R-parity conservation, the lightest supersymmetric particle is absolutely stable. The lightest supersymmetric particle is constrained to be a weakly interacting neutral particle [1].

In most of the supersymmetric models the lightest neutralino ($\tilde{\chi}_1^0$), which is typically an admixture of gauginos and higgsinos, is the lightest supersymmetric particle (LSP). Such an LSP is a good candidate for a particle dark matter [2]. From the point of view of experimental discovery of supersymmetry at a collider like the LHC, the LSP is the final product of the cascade decay of a SUSY particle. In this work we will assume that the LSP is the lightest neutralino and that it escapes the collider experiments undetected. The cascade chain will typically also contain other neutralinos ($\tilde{\chi}_j^0$, $j = 2, 3, 4$) as well as charginos ($\tilde{\chi}_i^{\pm}$, $i = 1, 2$). The charginos are an admixture of charged gauginos and charged higgsinos. The composition and mass of the neutralinos and charginos will play a key role in the search for supersymmetric particles. These properties determine also the time scale of their decays. The mass patterns of the neutralinos in models with different particle content, or with specific SUSY breaking patterns, were considered in some detail in [3,4].

Although most of the phenomenological studies involving neutralinos and charginos have been performed with universal gaugino masses at the grand unification scale, there is no compelling theoretical reason for such a choice. Gaugino masses follow from higher dimensional interaction terms which involve gauginos and auxiliary parts of chiral superfields in a given supersymmetric model. Assuming a $SU(5)$ grand unified theory (GUT) model, the auxiliary part of a chiral superfield in these higher dimensional terms can be in the representation **1**, **24**, **75**, or **200**, or some combination of these, of the underlying $SU(5)$ gauge group. If the auxiliary field of one of the $SU(5)$ nonsinglet chiral superfields obtains a vacuum expectation value (VEV), then the gaugino masses are not universal at the grand unification scale. Moreover, nonuniversal soft supersymmetry breaking masses, like gaugino masses, are a necessary feature in some of the supersymmetric models, e.g. in anomaly mediated supersymmetry breaking models the gaugino masses are not unified [5].

As indicated above, the phenomenology of supersymmetric models depends crucially on the composition of neutralinos and charginos. Thus, it is important to investigate the changes in the experimental signals for supersymmetry with the changes in the composition of neutralinos and charginos that may arise because of the changes in the underlying boundary conditions at the grand unification scale, or when the underlying supersymmetric model is changed. The implications of nonuniversal gaugino masses has been considered in a number of works, e.g. in a study of constraints arising from experimental measurements [6–8] and in the context of supersymmetric dark matter [9,10]. In [8], the decays of the second lightest neutralino were studied in the context of nonuniversal gaugino masses.

*Electronic address: Katri.Huitu@helsinki.fi
†Electronic address: jalaaman@pcu.helsinki.fi
‡Electronic address: ppandita@nehu.ac.in
§Electronic address: roy@pcu.helsinki.fi

In this paper we shall study the implications of the nonuniversal gaugino masses for the phenomenology of neutral Higgs bosons. It has been known for quite some time that the cascade decays of the SUSY particles may be a major source of the Higgs bosons [11–13]: the copiously produced strongly interacting particles can cascade decay to the Higgs bosons. In addition to the obvious interest in producing the Higgs bosons, it has been realized that this method of producing the Higgs bosons does not depend on the value of $\tan\beta$. Thus, this method of producing Higgs bosons may help to cover a larger parameter space as compared to the more conventional methods of studying the Higgs sector of supersymmetric models, including also the heavier Higgs bosons. The gauginos also play an important role in the decays of Higgs bosons when they are kinematically allowed to decay to the second lightest neutralino pair, which in turn may decay to the lightest neutralinos and two leptons [14]. Such a signal seems to be relatively easy to discover at the LHC [15,16]. We note here that Higgs boson production via cascade decays and detection via Higgs decay to neutralinos has been studied in CMS detector simulations at LHC [15–17] in the case of minimal supersymmetric standard model (MSSM) with universal gaugino masses. Here we study the Higgs production and decay when gaugino masses are nonuniversal.

The plan of the paper is as follows: In Sec. II we consider in detail the nonuniversality of gaugino masses as it arises in $SU(5)$ supersymmetric grand unified theory. In this section we consider analytically the implications of such a nonuniversality for neutralino and chargino masses. We derive sum rules involving the neutralino and chargino squared masses when the supersymmetry breaking gaugino masses are nonuniversal. In Sec. III we consider the phenomenology of Higgs bosons when the gaugino masses are nonuniversal. In this section we consider Higgs decays to heavier neutralinos which then cascade into the lightest neutralino and leptons. In Sec. IV we calculate the production of squark and gluino pairs in a particular scenario where the gluinos are heavier than squarks and then study the cascade decays of the squarks into Higgs bosons. We conclude our paper with a summary in Sec. V.

II. NONUNIVERSAL GAUGINO MASSES IN SUPERSYMMETRIC $SU(5)$

The masses and the compositions of neutralinos and charginos are determined by the soft supersymmetry breaking gaugino masses M_1, M_2, and M_3, corresponding to $U(1)$, $SU(2)$, and $SU(3)$ gauge groups, respectively, the supersymmetric Higgs mixing parameter μ, and the ratio of the vacuum expectation values of the two neutral Higgs bosons H_1^0 and H_2^0, $\langle H_2^0\rangle/\langle H_1^0\rangle = \tan\beta$. In the simplest supersymmetric models with universal gaugino masses, M_1, M_2, and M_3 are taken to be equal at the grand unified scale. However, in supersymmetric theories with an underlying grand unified gauge group, the gaugino masses need not be equal at the GUT scale. In this section we consider the nonuniversality of gaugino masses as it arises in the simplest of the supersymmetric grand unified theories, namely, supersymmetric $SU(5)$ grand unified theory, and its implications.

In grand unified supersymmetric models, including $SU(5)$ grand unified models, nonuniversal gaugino masses are generated by a nonsinglet chiral superfield Φ^n that appears linearly in the gauge kinetic function $f(\Phi)$ (the chiral superfields Φ are classified into a set of gauge singlet superfields Φ^s and gauge nonsinglet superfields Φ^n, respectively, under the grand unified group), which is an analytic function of the chiral superfields Φ in the theory [18]. If the auxiliary part F_Φ of a chiral superfield Φ in $f(\Phi)$ gets a VEV, then gaugino masses arise from the coupling of $f(\Phi)$ with the field strength superfield W^a. The Lagrangian for the coupling of gauge kinetic function to the gauge field strength is written as

$$\mathcal{L}_{\rm gk} = \int d^2\theta f_{ab}(\Phi) W^a W^b + \text{H.c.}, \tag{1}$$

where a and b are gauge group indices, and repeated indices are summed over. The gauge kinetic function $f_{ab}(\Phi)$ is

$$f_{ab}(\Phi) = f_0(\Phi^s)\delta_{ab} + \sum_n f_n(\Phi^s)\frac{\Phi^n_{ab}}{M_P} + \cdots, \tag{2}$$

where as indicated above the Φ^s and the Φ^n are the singlet and the nonsinglet chiral superfields, respectively. Here $f_0(\Phi^s)$ and $f_n(\Phi^s)$ are functions of gauge singlet superfields Φ^s, and M_P is some large scale. When F_Φ gets a VEV $\langle F_\Phi\rangle$, the interaction (1) gives rise to gaugino masses:

$$\mathcal{L}_{\rm gk} \supset \frac{\langle F_\Phi\rangle_{ab}}{M_P}\lambda^a\lambda^b + \text{H.c.}, \tag{3}$$

where $\lambda^{a,b}$ are gaugino fields. Note that we denote by λ_1, λ_2, and λ_3 the $U(1)$, $SU(2)$, and $SU(3)$ gauginos, respectively. Since the gauginos belong to the adjoint representation of $SU(5)$, Φ and F_Φ can belong to any of the following representations appearing in the symmetric product of the two **24** dimensional representations of $SU(5)$:

$$(\mathbf{24}\otimes\mathbf{24})_{\rm Symm} = \mathbf{1}\oplus\mathbf{24}\oplus\mathbf{75}\oplus\mathbf{200}. \tag{4}$$

In the minimal, and the simplest, case Φ and F_Φ are assumed to be in the singlet representation of $SU(5)$, which implies equal gaugino masses at the GUT scale. However, as is clear from the decomposition (4), Φ can belong to any of the nonsinglet representations **24**, **75**, and **200** of $SU(5)$, in which case these gaugino masses are unequal but related to one another via the representation invariants [19]. In Table I we show the ratios of resulting gaugino masses at tree level as they arise when F_Φ belongs to various representations of $SU(5)$. For definiteness, we shall study the case of each representation separately, although an arbitrary combination of these is obviously also allowed.

These results are consistent with the unification of gauge couplings

TABLE I. Ratios of the gaugino masses at the GUT scale in the normalization $M_3(\mathrm{GUT}) = 1$ and at the electroweak scale in the normalization $M_3(\mathrm{EW}) = 1$ at the one-loop level.

F_Φ	M_1^G	M_2^G	M_3^G	M_1^{EW}	M_2^{EW}	M_3^{EW}
1	1	1	1	0.14	0.29	1
24	−0.5	−1.5	1	−0.07	−0.43	1
75	−5	3	1	−0.72	0.87	1
200	10	2	1	1.44	0.58	1

$$\alpha_3^G = \alpha_2^G = \alpha_1^G = \alpha^G (\approx 1/25), \tag{5}$$

at the grand unification scale, where we have neglected the contribution of nonuniversality to the gauge couplings. Such contributions have little effect on the phenomenological aspects in which we are interested for this paper. Because of the renormalization group (RG) evolution we have at any scale (at the one-loop level) [20]

$$\frac{M_i(t)}{\alpha_i(t)} = \frac{M_i(\mathrm{GUT})}{\alpha_i(\mathrm{GUT})}. \tag{6}$$

Thus, at any scale we have

$$M_1 = \frac{5}{3}\frac{\alpha}{\cos^2\theta_W}\left(\frac{M_1(\mathrm{GUT})}{\alpha_1(\mathrm{GUT})}\right), \tag{7}$$
$$M_2 = \frac{\alpha}{\sin^2\theta_W}\left(\frac{M_2(\mathrm{GUT})}{\alpha_2(\mathrm{GUT})}\right), \qquad M_3 = \alpha_3\left(\frac{M_3(\mathrm{GUT})}{\alpha_3(\mathrm{GUT})}\right).$$

For the **24** dimensional representation of $SU(5)$, we then have

$$\frac{M_1}{M_3} = -\frac{1}{2}\left(\frac{5}{3}\frac{\alpha}{\cos^2\theta_W}\right)\left(\frac{1}{\alpha_3}\right), \qquad \frac{M_2}{M_3} = -\frac{3}{2}\left(\frac{\alpha}{\sin^2\theta_W}\right)\left(\frac{1}{\alpha_3}\right). \tag{8}$$

Similarly, for the **75** dimensional representation of $SU(5)$, we have

$$\frac{M_1}{M_3} = -5\left(\frac{5}{3}\frac{\alpha}{\cos^2\theta_W}\right)\left(\frac{1}{\alpha_3}\right), \qquad \frac{M_2}{M_3} = 3\left(\frac{\alpha}{\sin^2\theta_W}\right)\left(\frac{1}{\alpha_3}\right), \tag{9}$$

and for the **200** dimensional representation of $SU(5)$ we have

$$\frac{M_1}{M_3} = 10\left(\frac{5}{3}\frac{\alpha}{\cos^2\theta_W}\right)\left(\frac{1}{\alpha_3}\right), \qquad \frac{M_2}{M_3} = 2\left(\frac{\alpha}{\sin^2\theta_W}\right)\left(\frac{1}{\alpha_3}\right). \tag{10}$$

We can scale down these results to the electroweak scale by using the relevant renormalization group equations. At the electroweak scale we have the result $M_1 < M_2$ for the singlet representation, $|M_1| < |M_2|$ for the **24** and **75** representation, and $M_1 > M_2$ for **200** dimensional representation of $SU(5)$, respectively. The approximate values for the soft gaugino masses at the weak scale $M_i(\mathrm{EW})$ are shown in Table I. These are calculated using one-loop RG equations for the gaugino masses and the gauge couplings. Two-loop effect is to increase the M_1/M_2 ratio slightly.

In Fig. 1 we have shown the dominant component of the lightest neutralino (LSP) for the four representations as a function of $\tan\beta$ and $M_2(\mathrm{EW})$ for the value of soft supersymmetry breaking scalar mass $m_0(\mathrm{GUT}) = 1$ TeV. The values of μ used in the computations were determined by requiring the radiative electroweak symmetry breaking at the relevant scale. The universal trilinear coupling A_0 was set to zero at the GUT scale and the sign of the Higgs mixing parameter μ was set to $+1$, but the choice of the sign is not crucial to the composition of the lightest neutralino. The scan was done using the program SOFTSUSY [21] that uses two-loop RG β functions for the relevant parameters.

For the case of the singlet representation, the dominant component is always the bino, as expected. This is also true for the **24** dimensional representation of $SU(5)$. For the singlet case the experimental mass limit of the lighter chargino ($m_{\tilde{\chi}_1^\pm} > 103$ GeV if $m_{\tilde{\nu}} > 200$ GeV, $m_{\tilde{\chi}_1^\pm} > 45$ GeV if $m_{\tilde{\nu}} < 200$ GeV [22]) restricts the lower end of the M_2 range. In the **24** dimensional representation the lower end of the M_2 range is restricted by the lightest neutralino mass limit $m_{\tilde{\chi}_1^0} > 36$ GeV [22].

For the **75** dimensional representation of $SU(5)$, we have several possibilities. For the value of the soft parameter $m_0 = 1$ TeV, one has a bino LSP for small values of M_2, a wino LSP for slightly larger values of M_2, and a higgsino LSP for $M_2 \gtrsim 300$ GeV, all for a value of $\tan\beta \gtrsim 10$. In the case of **75** dimensional representation there exists a band of discontinuity in the $(M_2, \tan\beta)$ parameter space. For these values of parameters the lighter chargino mass becomes too light. The lower end of the M_2 range is restricted in this case by the experimental limit on the gluino mass.

As seen in Fig. 1, for the **200** dimensional representation the LSP is either a wino or a higgsino, depending on the values of M_2 and $\tan\beta$. Here, as in the singlet case, the experimental lightest chargino mass limit restricts the lower end of the M_2 range. Also in the **200** dimensional representation there is a small region around $7 \lesssim \tan\beta \lesssim 8$, $610\ \mathrm{GeV} < M_2(\mathrm{EW}) < 620$ GeV, where the experimental mass limits of charginos (and also neutralinos) are not met.

We recall here that there is a general upper bound on the mass of the lightest neutralino ($\tilde{\chi}_1^0$) that follows from the structure of the neutralino mass matrix [3,4]. This upper bound can be written as

$$M^2_{\tilde{\chi}_1^0} \leq \frac{1}{2}\Big(M_1^2 + M_2^2 + M_Z^2 - \sqrt{(M_1^2 - M_2^2)^2 + M_Z^4 - 2(M_1^2 - M_2^2)M_Z^2\cos 2\theta_W}\Big). \tag{11}$$

In Fig. 2 we plot this upper bound for the lightest neutralino

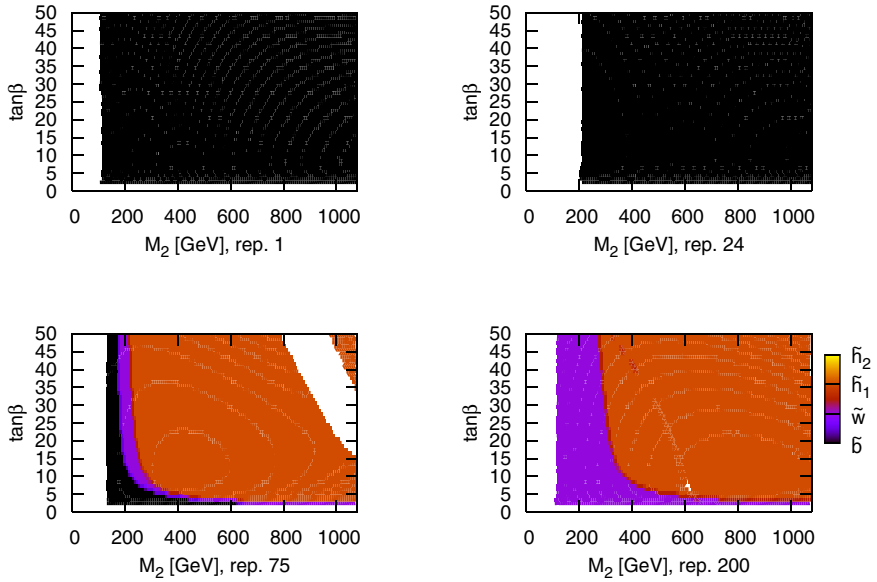

FIG. 1 (color online). Main component of the lightest neutralino in different representations of $SU(5)$ that arise in the product (4) for a common universal scalar mass $m_0 = 1$ TeV given at the GUT scale. The value of M_2 is calculated and plotted at the electroweak scale.

mass for the four different representations of $SU(5)$ that we have considered in this paper. From Fig. 2(a) we see that the large coefficients in the Table I result in large differences in the upper bound on the mass of the lightest neutralino for the four different representations in (4). Similarly, as discussed in [4], an upper bound can be obtained for the second lightest neutralino. This upper bound for $\tilde{\chi}_2^0$ is shown in Fig. 2(b). The gaugino masses here are calculated in the next-to-leading order (see e.g. [4]).

In order to study analytically the implications of the nonuniversal gaugino masses on the neutralino and chargino mass spectrum, we consider the trace of the neutralino and chargino mass squared matrices. From the trace of these matrices, we can calculate the average mass squared difference of the charginos and neutralinos. This mass squared difference depends only on the physical masses, and not on the Higgs(ino) mass parameter μ or the ratio of VEV's, $\tan\beta$ [20]. For the four different representations of $SU(5)$ which arise in (4), we find at the tree level the sum rules

$$M_{\rm sum}^2 = 2(M_{\tilde{\chi}_1^\pm}^2 + M_{\tilde{\chi}_2^\pm}^2) - (M_{\tilde{\chi}_1^0}^2 + M_{\tilde{\chi}_2^0}^2 + M_{\tilde{\chi}_3^0}^2 + M_{\tilde{\chi}_4^0}^2)$$

$$= (\alpha_2^2 - \alpha_1^2)\frac{M_{\tilde{g}}^2}{\alpha_3^2} + 4m_W^2 - 2m_Z^2, \quad \text{for } \mathbf{1}, \tag{12}$$

$$= \left(\frac{9}{4}\alpha_2^2 - \frac{1}{4}\alpha_1^2\right)\frac{M_{\tilde{g}}^2}{\alpha_3^2} + 4m_W^2 - 2m_Z^2, \quad \text{for } \mathbf{24}, \tag{13}$$

$$= (9\alpha_2^2 - 25\alpha_1^2)\frac{M_{\tilde{g}}^2}{\alpha_3^2} + 4m_W^2 - 2m_Z^2, \quad \text{for } \mathbf{75}, \tag{14}$$

$$= (4\alpha_2^2 - 100\alpha_1^2)\frac{M_{\tilde{g}}^2}{\alpha_3^2} + 4m_W^2 - 2m_Z^2, \quad \text{for } \mathbf{200}. \tag{15}$$

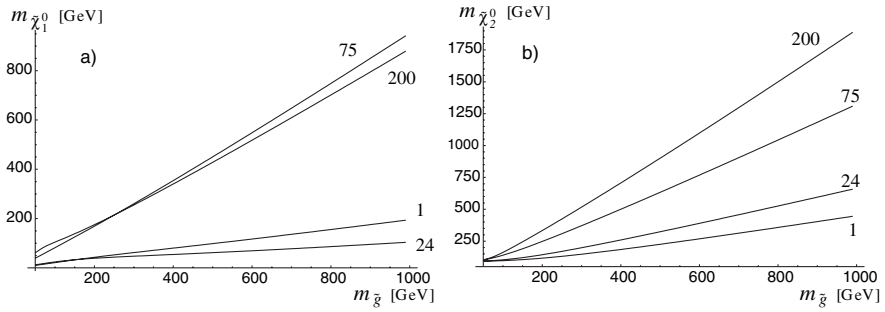

FIG. 2. The upper bound for (a) the lightest neutralino mass and (b) for the second lightest neutralino mass for different representations that arise in (4).

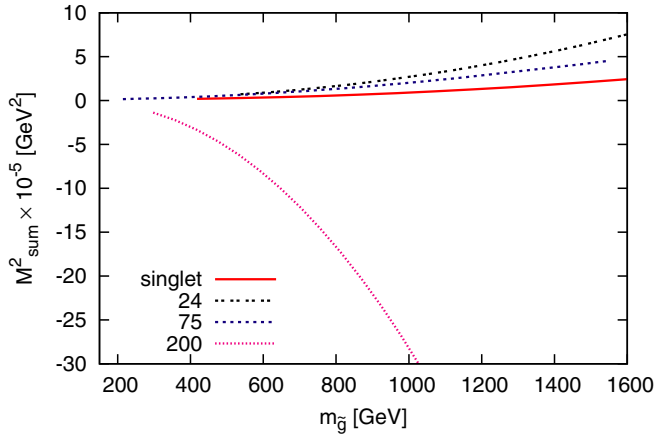

FIG. 3 (color online). The sum rule $2\sum m^2_{\tilde{\chi}^{\pm}_i} - \sum m^2_{\tilde{\chi}^0_i}$ as a function of the gluino mass.

From these sum rules we see that at the tree-level the average mass squared difference between charginos and neutralinos is positive for the representations **1**, **24**, and **75**, whereas for the representation **200** it is negative. In this respect the representation **200** resembles the anomaly mediated supersymmetry breaking scenario, where it was found that the average mass squared difference is negative [23]. In Fig. 3, we have plotted the above sum rules for the different $SU(5)$ representations that arise in (4). For the numerical evaluation of the masses, we have used the program SOFTSUSY [21], including radiative corrections to the neutralino and chargino masses.

III. HIGGS DETECTION USING H^0, $A^0 \to \tilde{\chi}^0_2\tilde{\chi}^0_2 \to 4l$

It is often assumed, when considering the detection of the Higgs bosons in supersymmetric models, that supersymmetric partners are too heavy so that Higgs bosons cannot decay into supersymmetric particles. However, it may well be that for the heavy Higgs bosons H^0, A^0, and $H^{\pm}$ the decays to supersymmetric particles are important or even dominant [15,16]. On the other hand, the decay branching ratios of neutralinos and charginos have been analyzed in [24]. In the case of large $\tan\beta$, when the couplings to the heavy fermions are enhanced, the decays to the third generation particles have been discussed in [25]. For large values of $\tan\beta$, the decays to the third generation particles for the nonuniversal gaugino masses were discussed in [8]. Here we are interested in Higgs decay to $\tilde{\chi}^0_2$, which in turn decays to electrons and muons in the case of nonuniversal gaugino masses.

A. Decay of $\tilde{\chi}^0_2$ to leptons

Of the supersymmetric particles, the light neutralinos $\tilde{\chi}^0_{1,2}$, the light chargino $\tilde{\chi}^{\pm}_1$, and the lightest sleptons are usually among the lightest particles in the spectrum. Higgs decays to sleptons are suppressed because of the small coupling, which is proportional to the corresponding lepton mass. The decay to the lightest neutralino LSP is among the invisible decays, which may be extremely difficult to detect at the LHC. In the minimal SUGRA model, the second lightest neutralino and the lighter of the charginos have similar mass. In [15], the decay of the heavy neutral Higgs boson to a pair of the second lightest neutralinos was studied. It was found that in the case when the branching ratio of $\tilde{\chi}^0_2$ to two leptons and the lightest neutralino is large, then the possibilities of detection are promising. Even though the branching ratio to a chargino pair may be larger [14,26], the decay to $\tilde{\chi}^0_2$'s is more promising because of the clear four lepton signal. We will, therefore, study the decay chain

$$H^0, A^0 \to \tilde{\chi}^0_2\tilde{\chi}^0_2, \qquad \tilde{\chi}^0_2 \to \tilde{\chi}^0_1 l^+ l^-, \qquad l = e, \mu \quad (16)$$

for the four different representations of $SU(5)$ in (4). The decay $\tilde{\chi}^0_2 \to \tilde{\chi}^0_1 l^+ l^-$ depends on the parameters M_2, M_1, μ, and $\tan\beta$, which control the neutralino masses and the mixing parameters, and also on the slepton masses $m_{\tilde{l}}$. As long as the direct decay of $\tilde{\chi}^0_2$ into $\tilde{\chi}^0_1 + Z^0$ is suppressed and the sleptons are heavier than the $\tilde{\chi}^0_2$, three-body decays of $\tilde{\chi}^0_2$ into charged leptons and $\tilde{\chi}^0_1$ will be significant. There can also be constructive or destructive interference between the Z^0 and the slepton exchange amplitudes which can have strong influence on the branching ratio. In some cases, we consider also the possibility that the sleptons mediating the decay $\tilde{\chi}^0_2 \to \tilde{\chi}^0_1 l^+ l^-$ can be on mass shell. Also, in order to have large branching ratios to the sleptons, they should be lighter than the squarks. This is usually true in SUSY models.

In the singlet case, the three-body decay $\tilde{\chi}^0_2 \to \tilde{\chi}^0_1 l^+ l^-$ was discussed in Ref. [15] for a particular set of parameters, for which the branching ratio is large. Here, all the sleptons (including the staus) are assumed to have soft SUSY breaking masses of 250 GeV and the value of $\mu = -500$ GeV. In this analysis M_2 is a free parameter, and its value at the electroweak scale is taken to be 150 GeV. The squark masses are all taken equal to 1 TeV. We also have taken a large value of the trilinear scalar coupling $A_t = 1$ TeV in order to have experimentally acceptable mass for the lightest Higgs boson. All the soft scalar masses, the value of A_t and the value of μ are taken at the electroweak scale. The pseudoscalar Higgs mass m_A is a free parameter and its value is taken to be 340 GeV. The value of M_1 is determined from the ratio of the gaugino mass parameters in the singlet representation of $SU(5)$ in (4). Because of the mentioned choice of M_2, $\tilde{\chi}^0_2$ is predominantly a wino, and $\tilde{\chi}^0_1$ is a bino-dominated state. The decay of $\tilde{\chi}^0_2$ into $\tilde{\chi}^0_1$ and a Z^0 is kinematically disallowed. The branching ratio of the three-body decay is shown in Fig. 4 as a function of $\tan\beta$ for the singlet case as well as for the representation **75**. We have calculated the branching ratio using the program SDECAY [27]. In this figure the initial value of $\tan\beta$ is 4.5,

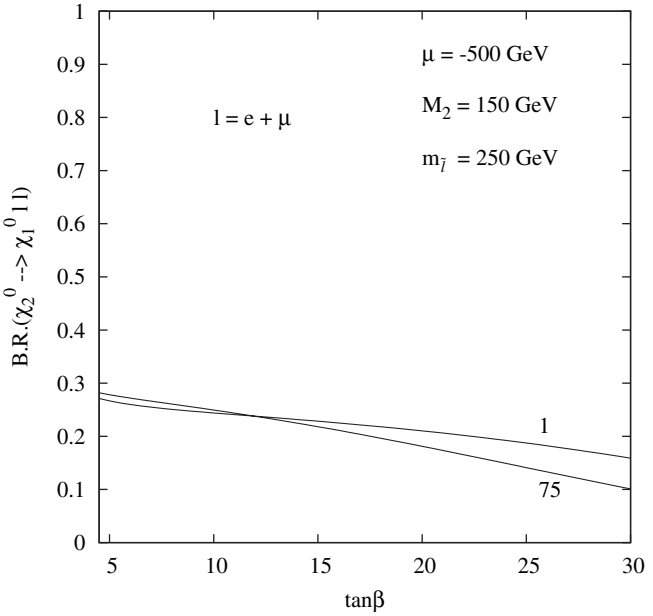

FIG. 4. Branching ratio as a function of $\tan\beta$ in the case of $m_{\tilde{l}} > m_{\tilde{\chi}_2^0}$ and for the representations **1** and **75**.

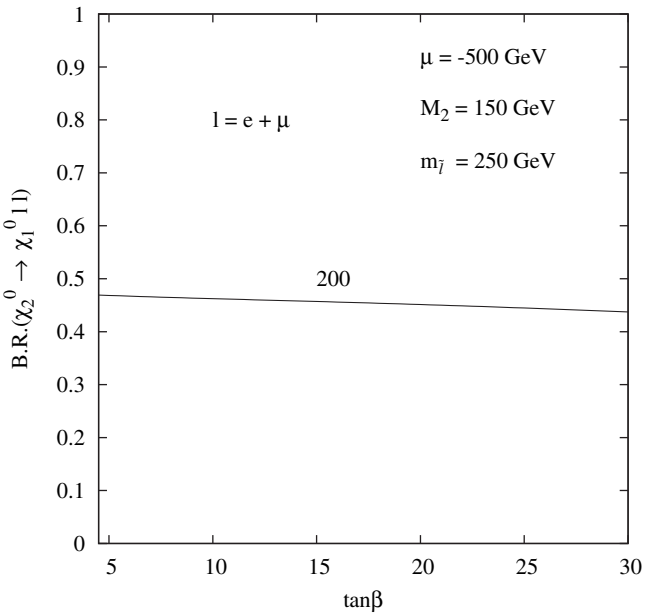

FIG. 5. Branching ratio as a function of $\tan\beta$, in the case of $m_{\tilde{l}} < m_{\tilde{\chi}_2^0}$, for the representation **200**. All other parameters are the same as in Fig. 4.

since for a lower value of $\tan\beta$ the light Higgs mass m_h is less than 114.4 GeV, which is the LEP lower limit [28]. We see from the figure that for higher values of $\tan\beta$ this branching ratio decreases since the branching ratio $\tilde{\chi}_2^0 \to \tilde{\chi}_1^0\tau^+\tau^-$ increases with $\tan\beta$ due to a larger Yukawa coupling.

For the representation **75**, $\tilde{\chi}_2^0$ is wino dominated and $\tilde{\chi}_1^0$ is bino dominated as in the singlet case. However, the mass difference between the $\tilde{\chi}_2^0$ and the $\tilde{\chi}_1^0$ is much smaller compared to the singlet case. As we see from Fig. 4, in the low $\tan\beta$ region the branching ratio for these two different representations are very close though the branching ratio for the **75** representation is slightly larger. This is due to the fact that $\mathrm{BR}(\tilde{\chi}_2^0 \to \tilde{\chi}_1^0 q\bar{q})$ is slightly larger in the singlet case as compared to the case of **75** dimensional representation. The leptonic branching ratio is then almost equally distributed among the available channels. However, for large $\tan\beta$ the branching ratio in the $\tilde{\chi}_1^0\tau^+\tau^-$ channel is larger for the **75** case than for the singlet case. For large $\tan\beta$ this makes the branching ratio in the $\tilde{\chi}_1^0 l^+ l^-$ channel smaller for the case of **75** dimensional representation. We also note that in the case of **75** dimensional representation the partial decay width of $\tilde{\chi}_2^0 \to \tilde{\chi}_1^0\nu\bar{\nu}$ is larger than the partial decay width of $\tilde{\chi}_2^0 \to \tilde{\chi}_1^0 l^+ l^-$ in the large $\tan\beta$ region. On the other hand, in the singlet case the partial decay width of $\tilde{\chi}_2^0 \to \tilde{\chi}_1^0\nu\bar{\nu}$ is always smaller than that of $\tilde{\chi}_2^0 \to \tilde{\chi}_1^0 l^+ l^-$.

For the set of parameters that we have discussed and in the case of the representation **200**, the spectrum is such that all the left- and right-handed sleptons are lighter than $\tilde{\chi}_2^0$ and are produced on mass shell. Although, $\tilde{l}_R$ proceeds with 100% branching ratio to $\tilde{\chi}_1^0 + l$, in the case of $\tilde{l}_L$ one should multiply by the appropriate branching fraction. This is shown in Fig. 5. One can see that the dependence on $\tan\beta$ is not significant in this case. The results for the representation **24** are not shown here due to the fact that it results in the lightest neutralino mass below the current experimental lower limit.

1. The case of **200**

In this subsection we will consider the representation **200** of $SU(5)$, as it arises in (4), in some detail. The ratio of the $U(1)$ and the $SU(2)$ gaugino masses is approximately given by (at the one-loop level[1])

$$|M_1|:|M_2| = 2.5{:}1. \tag{17}$$

This resembles very much the scenario of anomaly mediated supersymmetry breaking for values of μ larger than M_2. Let us now highlight two important characteristics of this representation.

(i) $\tilde{\chi}_1^\pm$ and $\tilde{\chi}_1^0$ are almost exclusively winos, and they are nearly degenerate in mass.

(ii) $\tilde{\chi}_2^0$ is predominantly a bino for $|\mu| > M_1$.

Consider the decay $\tilde{\chi}_2^0 \to \tilde{\chi}_1^0 l^+ l^-$ for the **200** dimensional representation. We again choose the scalar masses in

[1]Using the two-loop renormalization group equations (RGEs) the ratio is approximately 2.6:1 for a wide range of parameter choices. Similarly, for other representations the change in this ratio with the use of two-loop RGEs does not change our conclusions.

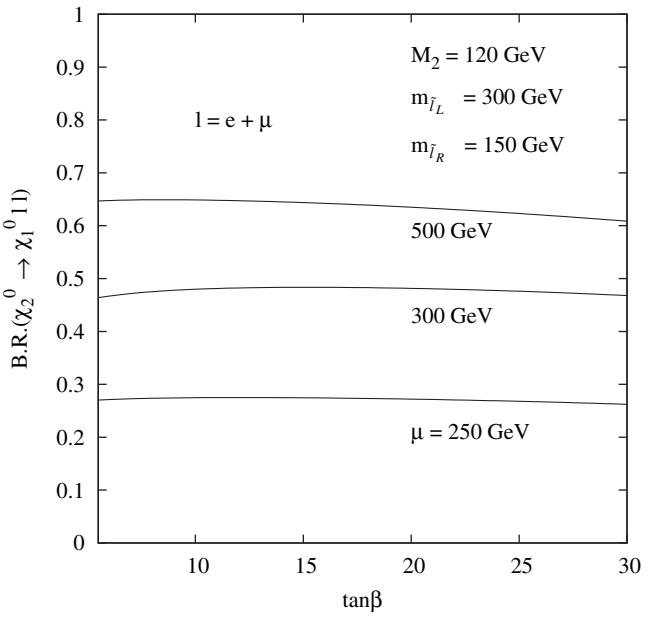

FIG. 6. Branching ratio as a function of $\tan\beta$ in the case of $m_{\tilde{l}_R} < m_{\tilde{\chi}_2^0}$ and for the representation **200** and for three different values of μ.

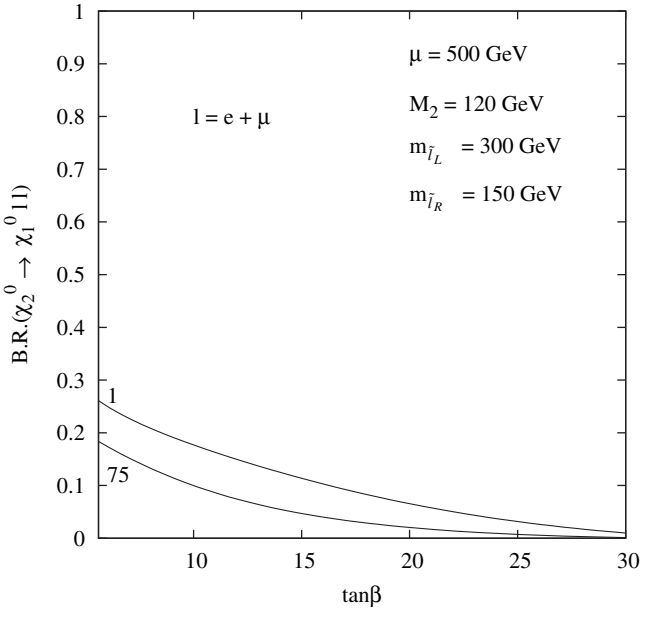

FIG. 7. Branching ratio as a function of $\tan\beta$ in the case of $m_{\tilde{l}} > m_{\tilde{\chi}_2^0}$ and for the representations **1** and **75** and for $\mu =$ 500 GeV. All other parameters are the same as in Fig. 6.

such a way that $m_{\tilde{l}_R}, m_{\tilde{\tau}_1} < m_{\tilde{\chi}_2^0} < m_{\tilde{l}_L}, m_{\tilde{\nu}}$. The reason for such a choice is that the two-body decay $\tilde{\chi}_2^0 \to \tilde{l}_R l$ is allowed. Although the decay of $\tilde{l}_R$ into $l + \tilde{\chi}_1^0$ is highly suppressed due to the very small bino component in $\tilde{\chi}_1^0$, $\tilde{l}_R$ will decay eventually in this mode with a one hundred percent branching ratio. Of course, one should be careful to consider the possibility of a displaced vertex in the decay of $\tilde{l}_R$. The BR($\tilde{\chi}_2^0 \to \tilde{\chi}_1^0 l^+ l^-$) calculated in this manner depends very strongly on μ (increases with increasing μ) since as μ increases $\tilde{\chi}_2^0$ becomes more and more binolike, and thus the partial decay widths of $\tilde{\chi}_2^0 \to \tilde{\chi}_1^{\pm} W^{\mp}$ and $\tilde{\chi}_2^0 \to \tilde{\chi}_1^0 h$ are suppressed and the partial decay width of $\tilde{\chi}_2^0 \to \tilde{l}_R l$ is enhanced. This makes the branching ratio into $\tilde{l}_R l$ mode larger for large values of μ. This is shown in Fig. 6. The branching ratio in the channel $\tilde{\chi}_2^0 \to \tilde{\chi}_1^0 Z$ is always very small for all values of $\tan\beta$.

We note that in the case of the **200** dimensional representation we use the constraint $m_{\tilde{\chi}_1^{\pm}} > 88$ GeV applicable for nearly mass degenerate lighter chargino and the lightest neutralino [29].

Let us now discuss the BR($\tilde{\chi}_2^0 \to \tilde{\chi}_1^0 l^+ l^-$) for this set of parameters for the representations **1** and **75**. We do not compare the case for the representation **24** here since for the parameter choice of this figure the **24** dimensional representation always produces a lightest neutralino with mass below the current experimental limit [22]. For this set of parameters the representations **1** and **75** give similar kinds of spectrum so that no two-body decays of $\tilde{\chi}_2^0$ are allowed. In Fig. 7 we show the branching ratio for these two representations as a function of $\tan\beta$ and for a value of $\mu = 500$ GeV.

2. The case of **24**

In this subsection we will consider the case of **24** dimensional representation where $|M_1| \approx 0.166|M_2|$. We look for a set of parameters such that the mass of the lightest neutralino is not below the current experimental lower limit as was the case in the previous subsections. For the present study we again consider the mass spectrum $m_{\tilde{\chi}_1^0} < m_{\tilde{l}_R} < m_{\tilde{\chi}_2^0}$. We have taken $M_2 = 750$ GeV and $\mu = -200$ GeV. For this choice of the parameters the lightest neutralino $\tilde{\chi}_1^0$ is mostly a bino with some higgsino admixture whereas the second lightest neutralino is higgsino dominated with very small wino and bino components. The soft masses for the left-sleptons are assumed to be 300 GeV, whereas those of the right-sleptons are taken to be 150 GeV. Other parameters such as squark masses and the trilinear scalar coupling A_t are the same as before. Once again we have taken the values of these parameters at the electroweak scale. With this set of parameters the following two-body decay channels are dominant: $\tilde{\chi}_2^0 \to \tilde{l}_R l$ and $\tilde{\chi}_2^0 \to \tilde{\tau}_1 \tau$. We have plotted the branching ratio of $\tilde{\chi}_2^0 \to \tilde{\chi}_1^0 l^+ l^-$ as a function of $\tan\beta$ in Fig. 8. We see from this figure that for some values in the low $\tan\beta$ region this branching ratio can be as large as 65%. For large values of $\tan\beta$, the BR($\tilde{\chi}_2^0 \to \tilde{\chi}_1^0 \tau^+ \tau^-$) dominates. Also, for this choice of parameters in the **1**, **75**, and **200** representations in (4) we always have a stau LSP which we do not consider in our R-parity conserving scenario.

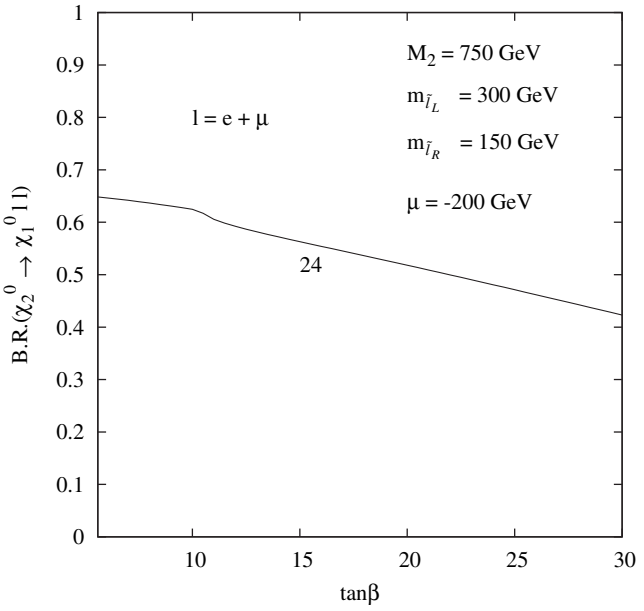

FIG. 8. Branching ratio as a function of $\tan\beta$ in the case of $m_{\tilde{l}_R} < m_{\chi_2^0}$ and for the representation **24**. The choice of other parameters is described in the text.

B. Decay of heavy Higgs bosons into a pair of neutralinos: $H^0, A^0 \to \tilde{\chi}_2^0\tilde{\chi}_2^0$

In this subsection we will study the branching ratios of the heavy Higgs bosons H^0 and A^0 into a pair of second lightest neutralinos. We have used the package HDECAY [30] to calculate the branching ratios. The decay widths and the branching ratios depend on the ratio of M_1 and M_2 along with other MSSM parameters. We have calculated the branching ratio of $H^0, A^0 \to \tilde{\chi}_2^0\tilde{\chi}_2^0$ for different $SU(5)$ representations that arise in the product (4). The coupling of the heavy Higgs boson H^0 with a pair of neutralinos is given by [31,32]:

$$H^0\tilde{\chi}_i^0\tilde{\chi}_j^0: -ig(A_L P_L + A_R P_R), \tag{18}$$

where $P_L = \frac{1}{2}(1-\gamma_5)$ and $P_R = \frac{1}{2}(1+\gamma_5)$ are the usual projection operators. The coefficients of P_L and P_R are given by

$$\begin{aligned} A_L &= Q_{ji}'^{*}\cos\alpha - S_{ji}''^{*}\sin\alpha, \\ A_R &= Q_{ij}''\cos\alpha - S_{ij}''\sin\alpha, \end{aligned} \tag{19}$$

where

$$\begin{aligned} Q_{ij}'' &= \frac{1}{2}[Z_{i3}(Z_{j2} - Z_{j1}\tan\theta_W) + Z_{j3}(Z_{i2} - Z_{i1}\tan\theta_W)]\epsilon_i, \\ S_{ij}'' &= \frac{1}{2}[Z_{i4}(Z_{j2} - Z_{j1}\tan\theta_W) + Z_{j4}(Z_{i2} - Z_{i1}\tan\theta_W)]\epsilon_i. \end{aligned} \tag{20}$$

Here Z is the neutralino mixing matrix in the basis $(-i\tilde{B}, -i\tilde{W}, \tilde{H}_1, \tilde{H}_2)$, and ϵ_i is the sign of the ith neutralino mass eigenvalue. Furthermore, $\sin\alpha$ and $\cos\alpha$ are the usual Higgs mixing angles.

Similarly, the coupling of the pseudoscalar Higgs boson A^0 to a pair of neutralinos is given by [31,32]:

$$A^0\tilde{\chi}_i^0\tilde{\chi}_j^0: -g(B_L P_L - B_R P_R), \tag{21}$$

where the coefficients of P_L and P_R are given by

$$\begin{aligned} B_L &= Q_{ji}'^{*}\sin\beta - S_{ji}''^{*}\cos\beta, \\ B_R &= Q_{ij}''\sin\beta - S_{ij}''\cos\beta. \end{aligned} \tag{22}$$

As an example, in Fig. 9, we have shown the dependence of branching ratio $\mathrm{BR}(H^0 \to \tilde{\chi}_2^0\tilde{\chi}_2^0)$ on m_A for a particular choice of MSSM parameters. This point in the parameter space is the same as in Fig. 7 with the choice of $\tan\beta = 6.5$. This way we can directly compare the branching ratios in the representations **1**, **75**, and **200**. In Fig. 10, we have plotted the branching ratio $\mathrm{BR}(A^0 \to \tilde{\chi}_2^0\tilde{\chi}_2^0)$ as a function of m_A for the same choice of parameters, and for the same $SU(5)$ representations. We can see that for this choice of the parameter set and for $m_A < 350$ GeV, the branching ratio of the decay of A^0 is larger than that of the decay of the heavy Higgs scalar H^0 for the representations **1** and **75**. This is due to the fact that for H^0 the total decay width is larger due to the increase in the number of available channels to the SM particles, which leads to a smaller branching ratio to sparticles. In the case of **200** dimensional representation the threshold opens up for heavier m_A, and once again the branching ratio of A^0 is larger than that of the H^0. As we have discussed earlier, the representation **24** produces a very light neutralino for this choice of parameters and is not further discussed here.

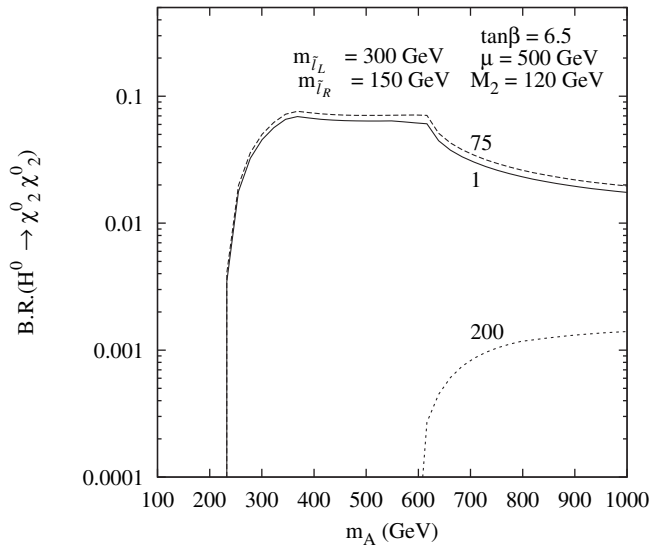

FIG. 9. The branching ratio of $H^0 \to \tilde{\chi}_2^0\tilde{\chi}_2^0$ as a function of m_A for three different $SU(5)$ representations in (4). Here $\tan\beta$ is taken to be 6.5, and other MSSM parameters are the same as in Fig. 7.

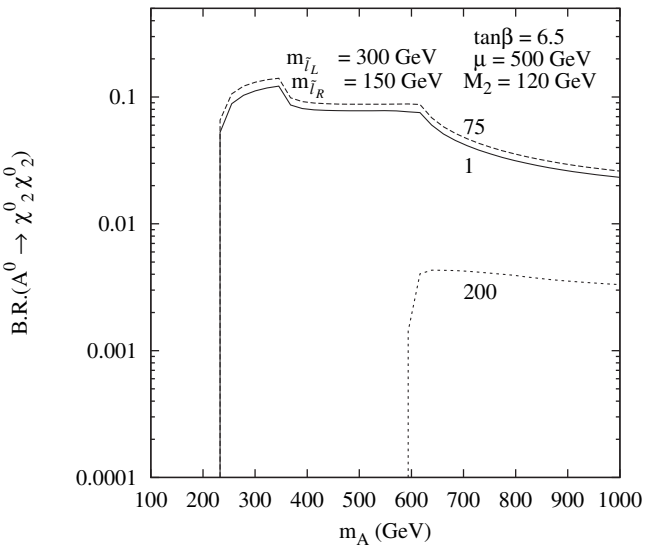

FIG. 10. The branching ratio of $A^0 \to \tilde{\chi}^0_2 \tilde{\chi}^0_2$ as a function of m_A for three different $SU(5)$ representations. Here, $\tan\beta$ is taken to be 6.5, and other MSSM parameters are the same as in Fig. 9.

C. Signal cross section

We now consider signal cross section and the total event rate in the four lepton channel at the LHC with $\sqrt{s} =$ 14 TeV for two different representations, the singlet and **75**. We show the contours of constant cross section in the (m_A, $\tan\beta$) plane for a representative set of MSSM parameters at the electroweak scale. As in Fig. 9, we have taken $\mu = 500$ GeV, $M_2 = 120$ GeV, all left slepton masses to be 300 GeV, and all the right slepton masses to be 150 GeV. All squark masses are taken to be 1 TeV. The top mass is $m_t = 178$ GeV and the bottom mass m_b is 4.25 GeV. The production cross section $gg \to H^0/A^0$ has been calculated in the next-to-leading order using the package HIGLU [33], which is based on the calculations in Ref. [34]. For the gluon distribution function we have used the distribution given in [35]. We note that for low values of $\tan\beta$ this channel dominates the production cross section. We also have considered the inclusive associated production $q\bar{q}$, $gg \to b\bar{b}H^0/A^0$ at the leading order [36] (which is essentially the leading order subprocess $b\bar{b} \to H^0/A^0$). The factorization and the renormalization scale are chosen to be $\mu_F = \mu_R = (m_{H/A} + 2m_b)/2$. The process $gg \to b\bar{b}H^0/A^0$ as well as the process $gg \to H^0/A^0$ is enhanced for larger values of $\tan\beta$ due to the large coupling of Higgs bosons to $b\bar{b}$. However, the process $gg \to b\bar{b}H^0/A^0$ dominates the production process for the values of m_A that we have considered here ($m_A \gtrsim 200$ GeV). In order to get a quantitative idea of these individual contributions to the Higgs boson production let us give an example here. If we take $\tan\beta = 20$ and $m_A = 230$ GeV then $gg \to H$ production cross section is 4.08 pb and $Hb\bar{b}$ production cross section is 31.4 pb at LHC energy. Next, we multiply these Higgs production cross sections by the appropriate branching ratios BR($H^0/A^0 \to \tilde{\chi}^0_2 \tilde{\chi}^0_2$) and BR($\tilde{\chi}^0_2 \to \tilde{\chi}^0_1 l^+ l^-$) discussed in the previous subsections in order to get the four lepton signal at the LHC. In Fig. 11 we have shown the contours of constant cross section of the $4l$ signal for the singlet representation arising in (4). We see that for $\tan\beta$ up to ≈ 10 and $m_A \sim 250$–350 GeV the total $4l$ cross section can reach up to 10 fb, which corresponds to 1000 signal events (without any cuts) for integrated luminosity of 100 fb^{-1}. In Fig. 12, the contours of constant cross section are shown for the representation **75** for the same choice of parameters. It is evident from this figure that a smaller region in the (m_A, $\tan\beta$) plane can be probed in this case with the same number of events. However, it shows different possibilities for these two representations. It is also evident from these two figures that the four lepton signal is very small for large values of $\tan\beta$ due to the suppression of the branching ratio BR($H^0/A^0 \to \tilde{\chi}^0_2 \tilde{\chi}^0_2$). In the case of the representation **200**, this four lepton signal is available only for higher values of m_A(>600 GeV) as can be seen from Figs. 9 and 10 for identical choices of other parameters. However, the total cross section is less than 1 fb for a large region in the (m_A–$\tan\beta$) plane and we do not show any separate plot for that. The total cross section in this four lepton channel can be similarly studied for the representation **24** for some different set of parameters which we do not pursue here.

We now briefly discuss the possible backgrounds to this four lepton signal. There can be two types of backgrounds, namely, the standard model processes leading to this type of signal, and SUSY processes. The main SM background comes from Z^0Z^0 and $t\bar{t}$ production. As discussed in Ref. [15], the $t\bar{t}$ background can be eliminated to a large

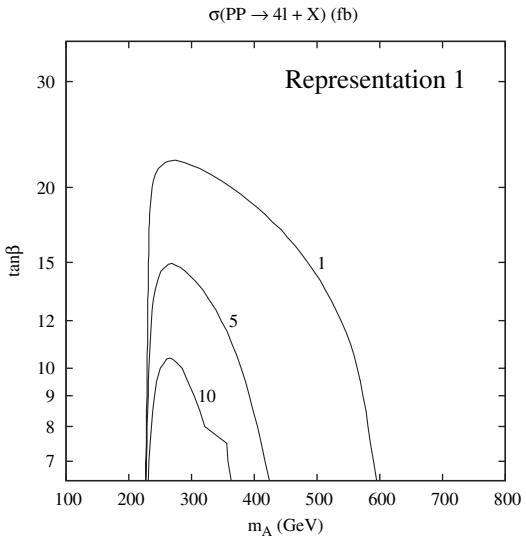

FIG. 11. Contours of $\sigma(pp \to H^0, A^0 \to \tilde{\chi}^0_2 \tilde{\chi}^0_2 \to 4l + X)\mu$ in fb, where $l = e^{\pm}$ or $\mu^{\pm}$ and X represents invisible final state particles. This is the case for the singlet representation. Other MSSM parameters are the same as in Fig. 9. $\sqrt{s} = 14$ TeV.

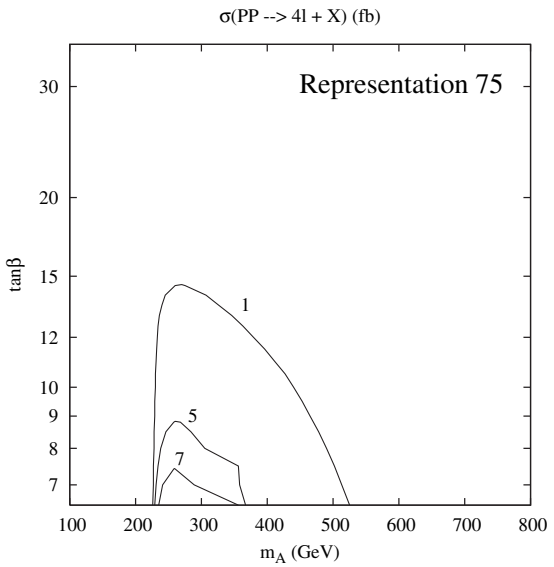

FIG. 12. Contours of $\sigma(pp \to H^0, A^0 \to \tilde{\chi}_2^0 \tilde{\chi}_2^0 \to 4l + X)$ in fb, where $l = e^{\pm}$ or $\mu^{\pm}$ and X represents invisible final state particles. This is the case for the representation **75**. Other MSSM parameters are the same as in Fig. 9. $\sqrt{s} = 14$ TeV.

extent by requiring four isolated leptons with $p_l^T > 10$ GeV. Demanding a missing transverse energy of 20 GeV and an explicit Z^0 veto can reduce the background from $Z^0 Z^0$. The background from SUSY processes can come from squark/gluino production or sneutrino pair production. The events coming from squark/gluino production can be eliminated by requiring soft jets with $E_T < 100$ GeV and $E_T^{\text{miss}} < 130$ GeV. The background coming from sneutrino pair production is more difficult to handle. However, it could possibly be distinguished due to the fact that it has larger E_T^{miss} and larger p_l^T compared to the signal. After using all these cuts the percentage of four lepton signal surviving is approximately about 60%. A detailed simulation of the signal and background events is beyond the scope of the present work. We hope to come back to this issue in a future work.

IV. HIGGS PRODUCTION IN THE CASCADE $\tilde{q}, \tilde{g} \to \tilde{\chi}_2^0 \to h\tilde{\chi}_1^0$

If squarks and gluinos are light enough to be produced ($pp \to \tilde{q}\tilde{q}', \tilde{g}\,\tilde{g}, \tilde{g}\,\tilde{q}$), then their production cross section will be large at a hadron collider. Thus, the decay chain

$$\tilde{q}, \tilde{g} \to \tilde{\chi}_2^0 + X \to \tilde{\chi}_1^0 h(H^0, A^0) + X \to \tilde{\chi}_1^0 b\bar{b} + X \quad (23)$$

will be an important source to look for Higgs bosons at LHC in the final state $b\bar{b}b\bar{b} + X$. This chain has been considered at LHC with universal gaugino masses in [12,16]. It was found that for suitable values of the parameters, the signal for all of the neutral Higgs bosons was clearly above the background. Discovery potential for A^0 and H^0 extended to 200 GeV, independent of the values of $\tan\beta$.

Here we will consider the decay chain in (23) for nonuniversal gaugino masses and study the changes that occur from the case of universal gaugino masses. We will only consider the cases without top squarks, which is enough to illustrate the differences that arise when the gaugino masses are nonuniversal.

In proton collisions, a squark pair, squark-antisquark, squark-gluino, or a gluino pair can be produced. We have used PROSPINO [37] to calculate the production cross sections of these modes (for $\sqrt{s} = 14$ TeV). Here we study the part of the parameter space for which $m_{\tilde{g}} > m_{\tilde{q}}$. Then every gluino decays to a quark and the corresponding squark. If the mass difference of the (top) squark and gluino is large enough then gluino may also decay to a top-stop pair. Because we are considering only the five lightest quark flavors, we have to remove top-stop contribution from the results.

In order to compare with the calculation in the universal (singlet) case in [12], we use the average branching ratios for particles, as used in [12], and which are defined in [38]. Thus we sum over all the decay widths of squarks decaying into a quark and a neutralino divided by the total decay width of squarks decaying into any neutralino and quark. The five squarks (excluding the stop) are considered to be equal in the sense that the bottom Yukawa coupling effect is neglected. The decay branching ratios are calculated using SDECAY [27] for squarks and neutralinos, and HDECAY [30] for the final decay of Higgs bosons to bottom quarks.

In Fig. 13(a) we have plotted the cross section of the decay chain (23) as a function of the gluino mass for the singlet representation. We have used parameters $\tan\beta = 10$, $m_A = 200$ GeV, $\mu = +500$ GeV, $m_{\tilde{q}} = 600$ GeV, and $m_{\tilde{l}} = 350$ GeV as low scale input values.

In the case of singlet representation, only the decay through the light Higgs boson h^0 is kinematically possible. The mass difference of the two lightest neutralinos is too small to produce heavier Higgs bosons H^0 and A^0. We can see a sharp rise in the cross section where the light Higgs channel opens up. This is due to an increase in the $\tilde{\chi}_2^0$ and $\tilde{\chi}_1^0$ mass difference as a function of the gluino mass. The production cross section of squarks decreases as gluino mass increases. This is of course independent of the representations arising in the product (4).

In Fig. 13(b) we have plotted the corresponding cross section for the **24** dimensional representation. Because of the changed relations between the gaugino mass parameters, the composition and masses of the neutralinos are different from the universal case. Now all the Higgs channels are available. We see that the CP-even neutral Higgs H^0 channel gives the largest cross section. As gluino mass increases, the decay branching ratio of $\tilde{\chi}_2^0 \to h, H^0, A^0 + \tilde{\chi}_1^0$ decreases.

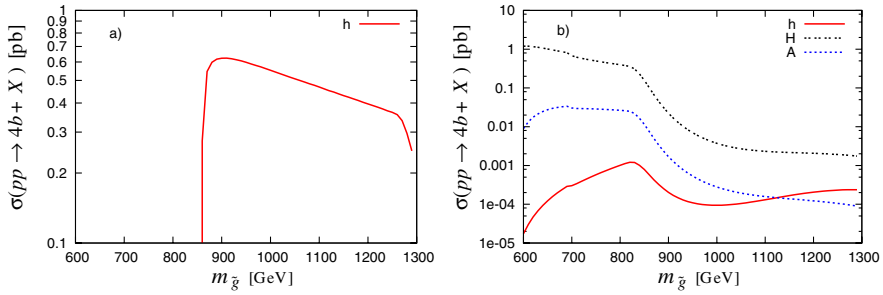

FIG. 13 (color online). Cross section $pp \to b\bar{b}b\bar{b} + X$ at LHC through the decay chain $\tilde{q}, \tilde{g} \to \tilde{\chi}_2^0 \to \tilde{\chi}_1^0 h(H^0, A^0) \to \tilde{\chi}_1^0 b\bar{b} + X$ for (a) the representation **1** via h, and (b) the representation **24** via h, H^0 and A^0.

In the **75** dimensional representation the mass difference of the two lightest neutralinos are generally too small in order for $\tilde{\chi}_2^0$ to decay into Higgs bosons, thereby making the decay chain, Eq. (23), irrelevant.

For the **200** dimensional representation, the mass difference of the two lightest neutralinos depends on the squark masses. Requiring the lightest neutralino to be the LSP, and for experimentally viable Higgs boson mass, the mass difference of the two lightest neutralinos is relatively small, and the total cross section resulting from the decay chain (23) remains below the detection level.

V. CONCLUSIONS

We have studied the consequences of gaugino mass nonuniversality as it arises in a supersymmetric grand unified theory for neutralino masses and mass relations, as well as for particular Higgs production and decay processes.

We found that the upper bounds of neutralino masses and the mass sum rules depend significantly on the representation. Similarly the studied decay possibilities of Higgs bosons depend on the representations. The decay of the second lightest neutralino to two leptons and the lightest neutralino very much depends on the mass difference between the lightest and second lightest neutralino which in turn depends on the representations. This is also true for the production of Higgs bosons in the decay of the second lightest neutralino.

From our considerations it seems clear that depending on the region of the parameter space, the Higgs decay $h(H^0, A^0) \to \tilde{\chi}_2^0 \tilde{\chi}_2^0$ may be observable for the gauginos emerging in any of the representations **1**, **24**, **75**, or **200** of $SU(5)$. However, the region in which $\tilde{\chi}_2^0 \to 2l + X$ is large, and it is possible for Higgs bosons to decay to the second lightest neutralinos, is rather limited in any of these models. Thus, the relevant regions of the parameter space do not necessarily overlap. In Sec. III we compared singlet and **75** using the same set of parameters. For **200**, the total cross section is less than 1 fb for the same choice of parameters when kinematically available. For the representation **24**, we did not find a region where a comparison could have been made.

Interestingly, for the production of the Higgs bosons via the decay chain including $\tilde{\chi}_2^0 \to h(H^0, A^0)\tilde{\chi}_1^0$, in addition to the singlet, we found relevant region of the parameter space only for the representation **24**. Furthermore, in this region the signal cross section for both neutral heavy Higgs bosons is reasonably large for not very heavy gluinos. It should be noted that in these two cases the signatures are clearly different. In the representation **24** the cross section is largest at the lighter values of the gluino mass for the heavy Higgses. For the lightest Higgs the production channel is open for all gluino masses in the representation **24** as opposed to the case of **1** representation. Also the fact that all the neutral Higgs channels are open in the **24** case distinguishes it from the singlet case, where only the light Higgs channel is available.

Finally, we note that it is possible to find similar signatures from the scenarios with nonuniversal Higgs masses [39].

ACKNOWLEDGMENTS

P. N. P. would like to thank the Helsinki Institute of Physics, where this work was initiated, for its hospitality. This work was supported by the Academy of Finland (Poject Nos. 104368 and 54023) and by the Council of Scientific and Industrial Research, India.

[1] M. Drees and M. Peskin "Proceedings of SUSY04 at Tsukuba, Japan" (http://www-conf.kek.jp/susy04/plenary.html).
[2] See, e.g. G. Jungman, M. Kamionkowski, and K. Griest, Phys. Rep. **267**, 195 (1996).
[3] P. N. Pandita, Phys. Rev. D **53**, 566 (1996).
[4] K. Huitu, J. Laamanen, and P. N. Pandita, Phys. Rev. D **67**, 115009 (2003).
[5] L. Randall and R. Sundrum, Nucl. Phys. **B557**, 79 (1999); G. F. Giudice, M. A. Luty, H. Murayama, and R. Rattazzi,

J. High Energy Phys. 12 (**1998**) 027.
[6] V. D. Barger and C. Kao,Phys. Rev. D **60**, 115015 (1999); G. Anderson, H. Baer, C.-H. Chen, and X. Tata, Phys. Rev. D **61**, 095005 (2000).
[7] K. Huitu, Y. Kawamura, T. Kobayashi, and K. Puolamäki, Phys. Rev. D **61**, 035001 (2000); G. Bélanger, F. Boudjema, A. Cottrant, A. Pukhov, and A. Semenov, Nucl. Phys. **B706**, 411 (2005).
[8] A. Djouadi, Y. Mambrini, and M. Mühlleitner, Eur. Phys. J. C **20**, 563 (2001).
[9] V. Bertin, E. Nezri, and J. Orloff, J. High Energy Phys. 02 (2003) 046; A. Birkedal-Hansen and B. D. Nelson, Phys. Rev. D **67**, 095006 (2003); U. Chattopadhyay and D. P. Roy, Phys. Rev. D **68**, 033010 (2003).
[10] A. Corsetti and P. Nath, Phys. Rev. D **64**, 125010 (2001).
[11] A. Bartl, W. Majerotto, and N. Oshimo, Phys. Lett. B **216**, 233 (1989); I. Hinchliffe, F. E. Paige, M. D. Shapiro, J. Söderqvist, and W. Yao, Phys. Rev. D **55**, 5520 (1997).
[12] A. Datta, A. Djouadi, M. Guchait, and F. Moortgat, Nucl. Phys. **B681**, 31 (2004).
[13] H. Baer, M. Bisset, X. Tata, and J. Woodside, Phys. Rev. D **46**, 303 (1992).
[14] H. Baer, M. Bisset, D. Dicus, C. Kao, and X. Tata, Phys. Rev. D **47**, 1062 (1993); H. Baer, M. Bisset, C. Kao, and X. Tata, Phys. Rev. D **50**, 316 (1994).
[15] S. Abdullin, D. Denegri, and F. Moortgat, CMS Report No. 2001/042 (2001).
[16] S. Abdullin *et al.*, CMS Report No. 2003/033 (2003).
[17] S. Abdullin *et al.*, CMS Report No. 1998-006,J. Phys. G **28**, 469 (2002).
[18] E. Cremmer, S. Ferrara, L. Girardello, and A. Van Proeyen, Phys. Lett. **116B**, 231 (1982).
[19] J. R. Ellis, K. Enqvist, D. V. Nanopoulos, and K. Tamvakis, Phys. Lett. **155B**, 381 (1985); M. Drees, Phys. Lett. **158B**, 409 (1985); G. Anderson *et al.*, *Proceedings of 1996 DPF/DPB Summer Study on New Directions for High Energy Physics (Snowmass 1996)*, hep-ph/9609457.
[20] S. P. Martin and P. Ramond, Phys. Rev. D **48**, 5365 (1993).
[21] B. Allanach, Comput. Phys. Commun. **143**, 305 (2002).
[22] S. Eidelman *et al.* (Particle Data Group), Phys. Lett. B **592**, 1 (2004).
[23] K. Huitu, J. Laamanen, and P. N. Pandita, Phys. Rev. D **65**, 115003 (2002).
[24] A. Bartl, H. Fraas, and W. Majerotto, Nucl. Phys. **B278**, 1 (1986).
[25] H. Baer, C. H. Chen, F. Paige, and X. Tata, Phys. Rev. D **58**, 075008 (1998); Phys. Rev. D **59**, 055014 (1999); Phys. Rev. Lett. **79**, 986 (1997); A. Bartl, W. Majerotto, and W. Porod, Phys. Lett. B **465**, 187 (1999).
[26] M. Bisset, N. Kersting, J. Li, S. Moretti, and F. Moortgat, hep-ph/0406152.
[27] M. Mühlleitner, A. Djouadi, and Y. Mambrini, hep-ph/0311167.
[28] R. Barate *et al.*, Phys. Lett. B **565**, 61 (2003).
[29] A. Heister *et al.* (ALEPH Collaboration), Phys. Lett. B **533**, 223 (2002).
[30] A. Djouadi, J. Kalinowski, and M. Spira, Comput. Phys. Commun., **108**, 56 (1998).
[31] J. F. Gunion and H. E. Haber, Nucl. Phys. **B272**, 1 (1986).
[32] S. Dawson, J. F. Gunion, H. E. Haber, and G. Kane, *The Higgs Hunter's Guide* (Addison-Wesley, Reading, Massachusetts, 1989).
[33] M. Spira, hep-ph/9510347.
[34] M. Spira, A. Djouadi, D. Graudenz, and P. M. Zerwas, Nucl. Phys. **B453**, 17 (1995).
[35] M. Glück, E. Reya, and A. Vogt, Z. Phys. C **53**, 127 (1992).
[36] D. A. Dicus and S. Willenbrock, Phys. Rev. D **39**, 751 (1989); M. Spira, Fortschr. Phys. **46**, 203 (1998); D. Dicus, T. Stelzer, Z. Sullivan, and S. Willenbrock, Phys. Rev. D **59**, 094016 (1999); F. Maltoni, Z. Sullivan, and S. Willenbrock, Phys. Rev. D **67**, 093005 (2003).
[37] W. Beenakker, R. Hopker, and M. Spira, hep-ph/9611232.
[38] A. Datta, A. Djouadi, M. Guchait, and Y. Mambrini, Phys. Rev. D **65**, 015007 (2002).
[39] H. Baer, A. Mustafayev, S. Profumo, A. Belyaev, and X. Tata, J. High Energy Phys. 07 (2005) 065.